www.serd.ait.ac.th/reric

Performance Analysis of Thermal Insulation Screens used for Classic Roofs in Hot-Humid Tropics

H. Abalo Samah* and Magolmèèna Banna*[1]

Abstract – *This work is devoted to the thermal performance evaluation of insulation materials used as screens in modern buildings in hot-humid areas. Average indoor air temperature, radiative cooling, heating loads and solar heat gain factors are calculated using dynamic nodal models established by taking into account air infiltration, leakage, and also air temperature stratification into the buildings. The numerical analysis developed is supplemented by an experimental work on test structures. Experimental and numerical results have proved that bioclimatic screens were better suitable to insulate the building from heat gain than thermal plaster screens, ground layers, and polystyrene plates. The laboratory work and numerical calculations have shown that the solar heat gain factor of the bioclimatic screen studied is less than 5%. The effect analysis carried out shows the importance and the role of flagstone roof thickness and the leaf area index (LAI), and hence the vegetable canopy type selection, on the thermal efficiency of the bioclimatic insulation screens. Results determine that larger LAI reduces the penetrating solar flux, the indoor air temperature and stabilizes the fluctuating values.*

Keywords – Bioclimatic insulation screen, heat transfer, modeling, simulation, thermal comfort.

1. INTRODUCTION

Thermal comfort has always been a primordial necessity in the life of human beings. Air-conditioning makes it possible to cure all or certain causes of discomfort and to give the buildings a suitable level of air moisture and temperature. Nowadays, this thermal comfort is obtained thanks to electric air-conditioning. This type of air-conditioning is penalized by energy crisis and environmental problems. In this context, research of passive air-conditioning systems becomes necessary. The purpose of the present study is to elaborate for engineers' simple computational tools to be used for passive air-conditioning buildings pre-designed in hot-humid tropics.

Gains through the building's fabrics occur due to the heating effect of absorbed solar radiation being conducted to the interior. This can be minimized by: the use of shading to reduce the amount of radiation falling on the building, the reduction of the absorbed radiation through the use of highly reflective finishes, the increase of the insulation value of the roof and walls. The estimation of the building's cooling energy takes into account the various thermal loads through the side walls, glazing, the air infiltrations and leakage, the building's internal gains (lighting, occupancy, electric equipment, etc.) and roof elements. For years, many works have shown the role of building materials, the hoods or fixed overhangs and building orientation on the improvement of thermal quality into the buildings. Certain works show that nearly 30 to 50% of heat gained inside the building is brought by the roof elements [1]. In hot tropical climate, thermal loads are more important and induce inside the buildings an unbearable indoor environment. It is thus essential to improve thermal quality into the buildings by reducing building's thermal loads. A priori, it is more rational to reduce the causes of heat load than to offset the heat load by increasing the cooling capability. Good thermal protection can greatly reduce the high thermal loads thereby improving thermal comfort in hot-humid tropics building. Thus the heat gain through the roof can be reduced by white paint, layers of wetted gunny bags [2]. Other techniques such as water pond with movable insulation, water spreading management and building shallow pond [1], [3] are also used. These techniques significantly improve thermal comfort in arid regions' buildings. The work of Xuxu [4] shows the interest and possibility of the establishment of thermal quality inside the buildings that use stabilized phase change materials at melting points close to ambient air. Because of their thermophysical properties these materials reduce temperature variations in the room. They absorb solar energy and melt during the day and then at night release energy stored during solidification in the air. The installation of thermal insulation screens underneath and above the roofs reduces the heat load in a building.

In hot-humid tropics, certain methods or techniques are better adapted to improve thermal quality inside the buildings.

Everyday experience shows that the solar heat load gained through roofs can be significantly reduced by incorporating a ceiling void or an attic space. Ventilating the void increases more the thermal resistance of void. This is backed up by theoretical analysis and laboratory work. The case study of Miranville [5] also confirmed that the heat load gained from a simple roof is greater than that gained from ceiling void or attic space. This work indicates that thin

*****Laboratoire Sur l'Energie Solaire / Groupe Phénomène de Transfert et Energétique, BP 1515 Faculté des Sciences, Université de Lomé, Togo.

[1]Corresponding author: Fax: (228) 221 85 95.
E-mail: magbanna@yahoo.fr.

reflective products between roof and ceiling minimize radiant heat load in attic space and reinforce thermal resistance of a complex roof.

External flora protect buildings from solar radiation in urban environment by offering aesthetically agreeable shadings, and providing a great reduction in local air temperature near canopy. Similarly, the flora establishes a comfortable microclimate in the areas and supply additional protection to the building from winds. In urban areas, the constraints related to space, lead to the establishment of green surface on the building's fabric, particularly on the roofs and side walls. The most prominent type of treatment might be planting vegetation in soil layer and creating green roof. Plants on roofs may contribute to offer a sustainable green surface by improving urban climate, minimising heat island effects, contributing to carbon sequestration and simultaneously protecting biodiversity. Green roofs present a very effective and positive impact on the urban climate and microclimate as well as on the indoor climate of buildings beneath them. In closed spaces with planted roofs, the air temperature beneath the plants during sunny time is lower than that of the air above. In fact, for their biological functions, such as photosynthesis, respiration, transpiration and evaporation, the foliage materials absorb a significant proportion of the solar radiation and contribute to reduce both cooling and heating loads of buildings in regions with large solar irradiation [6].

The thermal design of buildings depends on the indoor conditions requirements, the outdoor prevailing climatic conditions (ambient temperature, relative humidity, and total radiation), the infiltrations or the air leakage. It also depends on construction materials and insulation. The goal of this work is to develop mathematical heat transfer models for classic roofs integrating thermal insulation screens suitable in the tropical climatic zone. The objective is to propose simple dynamic nodal models which make it possible to take into account air infiltrations and temperature stratification inside the buildings. The present work aims to evaluate and compare the daily variations of useful parameters such as dynamic solar heat gains factor (SHF) which in the best of the cases must be less than 4%, and control parameters as radiant cooling and heating loads through various roofs insulation screens.

2. MATHEMATICAL FORMULATION

The physical models considered for heat transfer modeling are patios or test structures representing classic rooms drawn on a scale of 1/4. The models presented have taken into account different parts of the building: classic roofs (galvanized sheet, tile, and flagstone), indoor air zone, underground which is supposed to be at 30 m of depth and at (27°C). The patio has an internal height of 0.985m (floor-ceiling). Figure 1 schematizes the physical models chosen for classic roofs. The studied zone is divided into N isothermal elements with different thickness and physical properties that entail N0 non identical sublayers of the complex roof and 10 identical sublayers of indoor air zone. The outside surface is exposed to incident solar radiation (ϕ_β), convection heat transfer and radiation exchange with the sky. The inside surface of the roof is subject to combined convection, radiation and conduction heat. Generally, transfers into a room are much more complex because of being carried out in three dimensions (3D) space and time. The mathematical model is formulated by using the main following assumptions:

- The moisture of the air is nearly constant inside the room,
- The air is perfectly transparent in the infra-red radiation,
- The side walls of the patios are adiabatic,

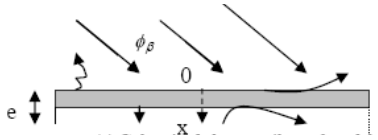

(a) Galvanized sheet or tile roof model

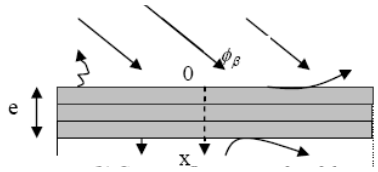

(b) Concrete flagstone roof model

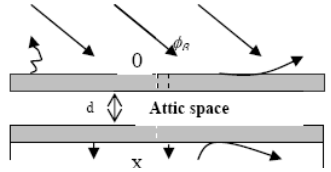

(c) Thin sheet roof with ceiling

Fig. 1. Model of classic roofs.

Based on the above assumptions, the thermal-network models are drawn up and the equations of transfers are written:

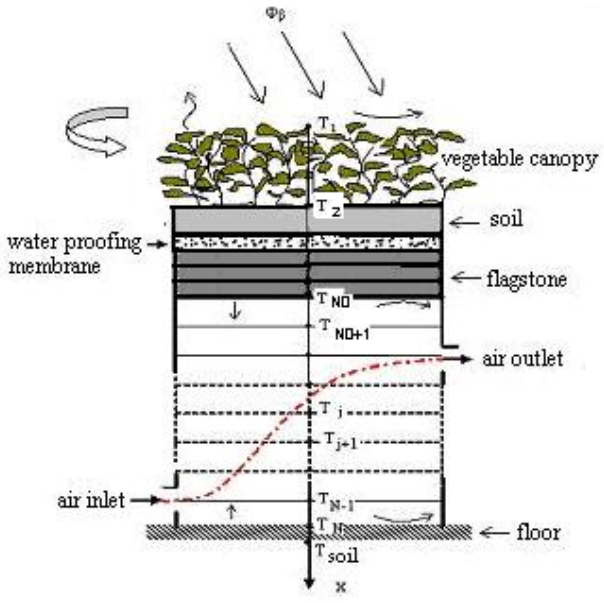

Fig. 2. Model of planted roof integrated to the building.

Simple classic roofs

- Galvanized sheet or tile roofs are discretized in two isothermal subjacent sublayers (N0=2) and the energy balance equations of the elements are:

$$e_1(\rho c_p)_1 \frac{\partial T_1}{\partial t} = \alpha\phi_\beta - h_{ae}(T_1 - T_a) - h_{rae}(T_1 - T_{sky}) - G_1(T_1 - T_2) \quad (1)$$

$$e_{N0}(\rho c_p)_{N0} \frac{\partial T_{N0}}{\partial t} = G_{N0-1}(T_{N0-1} - T_{N0}) - h_{N0}(T_{N0} - T_{N0+1}) - G_{N0}(T_{N0} - T_{N0}) - h_{rN}(T_{N0} - T_N) \quad (2)$$

- Cement flagstone roofs are discretized in four isothermal sublayers (N0=4) and the energy balance equations of the elements are:

$$e_1(\rho c_p)_1 \frac{\partial T_1}{\partial t} = \alpha\phi_\beta - h_{ae}(T_1 - T_a) - h_{rae}(T_1 - T_{sky}) - G_1(T_1 - T_2) \quad (3)$$

$$e_j(\rho c_p)_j \frac{\partial T_j}{\partial t} = G_{j-1}(T_{j-1} - T_j) - G_j(T_j - T_{j+1}) \quad j=2,3 \quad (4)$$

$$e_{N0}(\rho c_p)_{N0} \frac{\partial T_{N0}}{\partial t} = G_{N0-1}(T_{N0-1} - T_{N0}) - h_{N0-1}(T_{N0-1} - T_{N0}) - G_{N0-1}(T_{N0-1} - T_{N0}) - h_{rN}(T_{N0} - T_N) \quad (5)$$

- Indoor air zone is, in each configuration, discretized in 10 identical and isothermal sublayers for which heat transfer equations are written:

$$e_j(\rho c_p)_j \frac{\partial T_j}{\partial t} = h_{j-1}(T_{j-1} - T_j) + G_{j-1}(T_{j-1} - T_j) - h_j(T_j - T_{j+1}) - G_j(T_j - T_{j+1}) - (c_p \dot{m}/S)_j(T_{sj} - T_{ej})$$

j=N0+1, N-1 (6)

Floor interacts with the roof and indoor; its energy balance equation is:

$$e_N(\rho c_p)_N \frac{\partial T_N}{\partial t} = h_{N-1}(T_{N-1} - T_N) + G_{N-1}(T_{N-1} - T_N) - G_N(T_N - T_{sol}) + h_{rN}(T_{N0} - T_N) \quad (7)$$

Heat insulation screens for classic roofs

Heat gains induced by certain types of insulation materials suitable for classic roofs have been implemented. However, other heat insulation screens like the ground layer and bioclimatic vegetable covers screens on the classic cement flagstones can be used.

Ceiling void for thin sheeting roofs

Ceiling void or attic space commonly used in tropical zone as heat insulation screens is integrated to thin sheeting roof buildings and allows to maintain a void ventilated naturally or artificially between the roof and the ceiling. Figure 1c shows the physical model of ventilated attic. In the model, thin sheeting roof with ceiling void screen is discretized in five isothermal subjacent sublayers (N0=5) and transfer equations are written:

$$e_1(\rho c_p)_1 \frac{\partial T_1}{\partial t} = \alpha\phi_\beta - h_{ae}(T_1 - T_a) - h_{rae}(T_1 - T_{sky}) - G_1(T_1 - T_2) \quad (8)$$

$$e_2(\rho c_p)_2 \frac{\partial T_2}{\partial t} = G_1(T_1 - T_2) - h_2(T_2 - T_3) - G_2(T_2 - T_3) - h_{rN0}(T_2 - T_4) \quad (9)$$

$$e_3(\rho c_p)_3 \frac{\partial T_3}{\partial t} = h_2(T_2 - T_3) + G_2(T_2 - T_3) - h_3(T_3 - T_4) - G_3(T_3 - T_4) - (c_p \dot{m}/S)_3(T_{s3} - T_{e3}) \quad (10)$$

$$e_4(\rho c_p)_4 \frac{\partial T_4}{\partial t} = h_3(T_3 - T_4) + G_3(T_3 - T_4) + h_{rN0}(T_2 - T_4) - G_4(T_4 - T_5) \quad (11)$$

$$e_{N0}(\rho c_p)_{N0} \frac{\partial T_{N0}}{\partial t} = G_{N0-1}(T_{N0-1} - T_{N0}) - h_{N0}(T_{N0} - T_{N0+1}) - G_{N0}(T_{N0} - T_{N0+1}) - h_{rN}(T_{N0} - T_N) \quad (12)$$

Transfer equations for indoor air are identical to the preceding ones.

Insulation screens for concrete flagstone roofs

Thermal performances of certain screens used for reinforced concrete flagstone roofs are studied in particular extruded or moulded polystyrene plates, plaster false ceiling, ground layer and vegetable covers. Technically, these insulation screens are integrated beneath reinforced concrete flagstone as an insulation additional sublayer.

Polystyrene or plaster

The complex roof, associating polystyrene plate or plaster layer is discretized in five isothermal sublayers (N0=5) and transfer equations are written:

$$e_1(\rho c_p)_1 \frac{\partial T_1}{\partial t} = \alpha\phi_\beta - h_{ae}(T_1 - T_a) - h_{rae}(T_1 - T_{sky}) - G_1(T_1 - T_2) \quad (13)$$

$$e_j(\rho c_p)_j \frac{\partial T_j}{\partial t} = G_{j-1}(T_{j-1} - T_j) - G_j(T_j - T_{j+1})$$

$$j = 2, ..., 4 \quad (14)$$

$$e_{N0}(\rho c_p)_{N0} \frac{\partial T_{N0}}{\partial t} = G_{N0-1}(T_{N0-1} - T_{N0})$$

$$- h_{N0}(T_{N0} - T_{N0+1}) - G_{N0}(T_{N0} - T_{N0+1})$$

$$- h_{rN}(T_{N0} - T_N) \quad (15)$$

Ground layer

Technically, water proofing membrane is placed under ground layer. The complex roof is discretized in six isothermal sublayers (N0=6) and transfer equations are written:

$$e_1(\rho c_p)_1 \frac{\partial T_1}{\partial t} = \alpha\phi_\beta - h_{ae}(T_1 - T_a) - h_{rae}(T_1 - T_{sky})$$

$$-G_1(T_1 - T_2) \quad (16)$$

$$e_j(\rho c_p)_j \frac{\partial T_j}{\partial t} = G_{j-1}(T_{j-1} - T_j) - G_j(T_j - T_{j+1})$$

$$j = 2, ..., 5 \quad (17)$$

$$e_{N0}(\rho c_p)_{N0} \frac{\partial T_{N0}}{\partial t} = G_{N0-1}(T_{N0-1} - T_{N0})$$

$$- h_{N0}(T_{N0} - T_{N0+1}) - G_{N0}(T_{N0} - T_{N0+1})$$

$$- h_{rN}(T_{N0} - T_N) \quad (18)$$

Vegetable canopy

A green roof system can provide shading and protection from solar radiation and minimise the building's energy consumption in hot climatic areas. From ground screen, vegetable cover insulation screen is obtained by associating greenery. Many of studies predict thermal performance of stand-alone green roof localized to experimental site or employ several numerical techniques to evaluate thermal performance. This restricts the applicability of the green roof to particular buildings and hence thermal space conditioning of different building cannot be predicted, as green roof model is to be coupled to building simulation code. Effect of parametric variations in thermal components of green roof on cooling potential is not described. This model improves upon these aspects by incorporating thermal modeling of green roof components, parametric variations in the green roof components and coupling the model to the building simulation code.

The objective of studying green roof is multifold: to determine the effect of variations in foliage characteristics, viz. leaf area index (LAI) and the foliage height thickness on thermal performance of green canopy, estimation of thermal load reduction in the building and evaluation with thermal shading on building space conditioning.

Vegetable cover interacts with ambient air and wet ground placed on a water proofing membrane (sealing plastic) recovering the reinforced concrete flagstone. Incident solar radiation on the leaf area is partially reflected and absorbed by the sheets to provide the biological functions of the plants. The remainder of the solar radiation is absorbed by the wet ground which makes possible the evaporation of water.

Planted roof is discretized in seven isothermal sublayers (N0=7) and transfer equations are written:

$$e_1(\rho c_p)_1 \frac{\partial T_1}{\partial t} = \alpha_1\phi_{net}(\frac{e}{2}) + \frac{LAI}{1-\varepsilon_p} \frac{\rho c_p}{\gamma(r_i + r_e)}(P_{vs} - P_v)$$

$$-h_{rae}(T_1 - T_{sky}) - h_{ae}(T_1 - T_a) - G_1(T_1 - T_2) + L_v\Delta\dot{m} \quad (19)$$

$$e_2(\rho c_p)_2 \frac{\partial T_2}{\partial t} = G_1(T_1 - T_2) - G_2(T_2 - T_3) +$$

$$\alpha_2\phi_{net}(e_1) - L_v\Delta\dot{m} \quad (20)$$

$$e_j(\rho c_p)_j \frac{\partial T_j}{\partial t} = G_{j-1}(T_{j-1} - T_j) - G_j(T_j - T_{j+1})$$

$$j = 3,\ldots,6 \quad (21)$$

$$e_{N0}(\rho c_p)_{N0} \frac{\partial T_{N0}}{\partial t} = G_{N0-1}(T_{N0-1} - T_{N0})$$

$$-G_{N0}(T_{N0} - T_{N0+1}) - h_{N0}(T_{N0} - T_{N0+1})$$

$$-h_{rN}(T_{N0} - T_N) \quad (22)$$

Transfer equations for indoor air are identical to the preceding ones.

3. NUMERICAL SOLUTION PROCEDURE AND CONTROL PARAMETERS

Transfer equations are discretized by using the full implicit finite-differences method. The results are presented in linear matrix systems form: $[A]\{T\} = \{B\}$. The resolution of the systems is made by using Gauss-Seidel iterative method after the triangulation process of the linear equations. Natural convective and radiative heat transfer coefficients used in the equations are deduced from the classic relations [3]. The conductances are calculated as the ratio of the thermal conductivity to conduction layer thickness. The saturation vapor pressure is related to the sheet surface temperature [7].

The determination of temperature variations has allowed deducing useful parameters such as: solar heat gains factor (SHF), radiative cooling (R-value), average heat gains and indoor air temperature:

- Solar heat gain factor (SHF) of a roof is defined as the heat flow rate through the construction due to solar radiation expressed as a fraction of the incident solar radiation i.e. ratio of (transmitted solar energy) for zero air temperature differences to (incident solar energy):

$$SHF = (\varphi_e / \phi_\beta).100\%$$

This is a useful parameter to indicate the insulation of the roofs against solar gains through the fabric.

- Radiative cooling is the long wavelength radiation heat loss to ambient or sky and is expressed from the following relation [8]:

$$R\_value = \sigma\varepsilon_{roof}(T_1^4 - C_a\varepsilon_{sky}T_a^4)$$

where ε_{roof} is the emissivity of the roof, C_a is the cloudiness coefficient that can be deducted from the following relation:

$$C_a = 1 + 0.0224n - 0.0035n^2 + 0.00028n^3,$$

n is the total opaque cloud amount (0 for clear sky, 10 for overcast sky). The sky's emissivity is given by the expression:

$$\varepsilon_{sky} = 0.711 + 0.56(T_{dp}/100) + 0.37(T_{dp}/100)^2$$

The dew point temperature, T_{dp} is evaluated by the relation:

$$T_{dp} = C_3 \frac{\ln(RH) + C_1}{C_2 - (\ln(RH) + C_1)}$$

where $C_2 = 17.08085$ and $C_3 = 234.175$ and RH is the relative air humidity ranging from 0 to 1.

- Average indoor temperature is calculated by using Simpson numerical method:

$$T_M(t) = \left(\int_0^H T(x,t)dx\right) / H$$

- Average heat gains are calculated by taking into account only the heat load through roofs, the side walls being insulated. They are expressed from the following relation:

$$Q = \sum_{k=6h}^{18h} SHF.\phi_\beta(k).S.\Delta t$$

4. EXPERIMENTAL SETUP AND PROCEDURE

To determine the impact of the experimental passive cooling roof elements, measures are carried out under meteorological conditions at the laboratory in Lome (Togo) in November 2007. Each test patios is equipped with a network of type E thermocouples placed in different locations as shown in Figure 2. Two thermocouples are used for the thin roofs (top and bottom surface), four thermocouples are used for the reinforced concrete flagstone (top surface, 2 middle points, bottom surface). Four other thermocouples are distributed along the patio internal height in order to check indoor air temperature stratification. A common thermocouple was used to measure out ambient air temperature. The thermocouples were placed and handled with care to ensure proper temperature data.

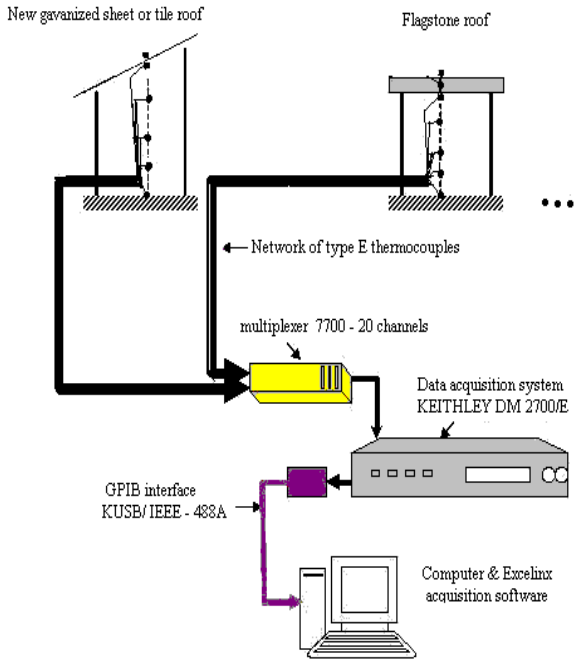

Fig. 3. Experimental device: schematic view of instruments and test structures.

These thermocouples make it possible to measure a range of temperature ranging from -200°C to +1000°C with an absolute uncertainty lower than 1°C, for the gap of temperature going from 0°C to +70°C. The thermocouples are calibrated at the laboratory using a bath of melting ice at 0°C and a bath controlled in temperature. The acquisition chain included a network of thermocouples, 20 channel multiplexer 7700, KEITHLEY DM2700/E data acquisition system integrating the IEEE card, GPIB interface using KUSB-488A port and a micro computer. The temperature measurement is carried out with an accuracy of 0.5 degree. Data processing is carried out using Excelinx acquisition software. Global solar radiation on a horizontal plan is recorded using a pyranometer and data Logger. Wind velocity is measured by a hot wire anemometer TESTO 425 which provides values with an accuracy of 5%.

5. RESULTS AND DISCUSSIONS

Numerical calculations have been performed corresponding to the hourly variation of global solar radiation and ambient air temperature on typical dry season day (November) in Lome. These meteorological data are used as inputs to the program. Solar energy reaches a maximum value of 750 W/m^2 at 12 noon whereas the maximum air ambient temperature reaches a maximum of 307 K at 1 pm, with one hour delay time. The wind speed and air humidity remain nearly stable with average values respectively of 3 m/s and 68% during the experiment days.

Classic roofs' thermal response

Simulation and the experimental process were allowed to show clearly the effect of the stratification of the indoor air temperature inside buildings. This phenomenon was also observed by Runsheng Tang [9]

in the case of vaulted roofs. Temperatures decrease from the roof to the floor in the morning; but in the night, the phenomenon is naturally reversed as shown on Figure 4. In spite of the fluctuations in measured temperatures, the experimental and numerical variations have the same mean temporal evolution pattern.

As shown in Figure 5, the thin sheeting roofs have a low thermal inertia and a significant proportion of solar energy is quickly transferred into the room degrading considerably thermal quality inside buildings.

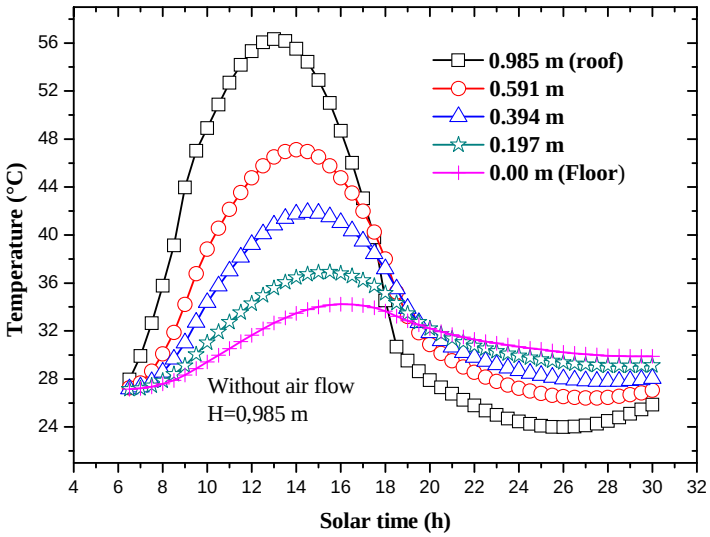

Fig. 4a. Indoor air temperature stratification inside building -theoretical curves.

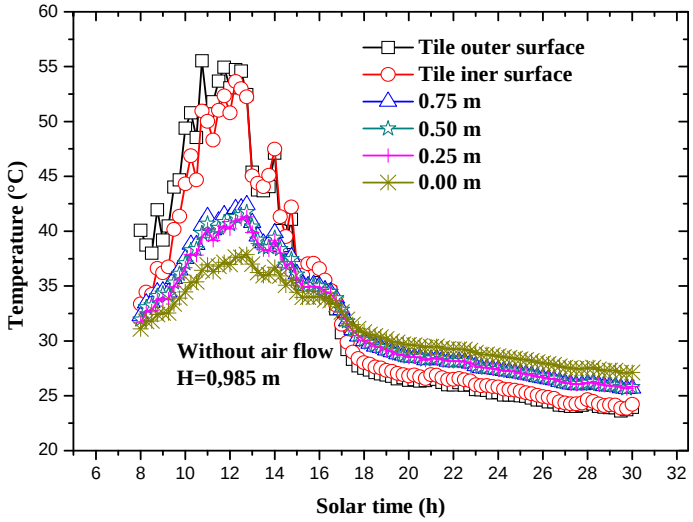

Fig. 4b. Indoor air temperature stratification inside building - experimental curves.

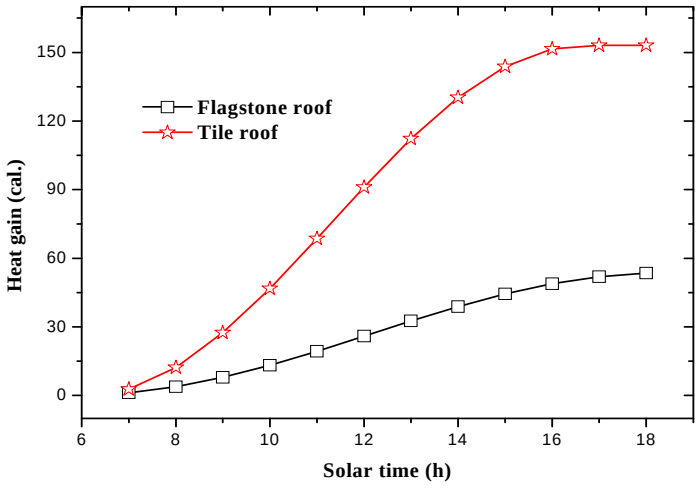

Fig. 5. Daily variation of heat gains of patios in classic.

Figure 6 illustrates that the warming has reached its maximum around 2.p.m. (solar time) in spite of the long wavelength radiation losses (Figure 7). On the other hand, for the reinforced concrete flagstone, the warming is less in the morning, compared to the cases of the thin sheeting roof. However, as shown by Sami [10], the high temperatures persist even later in the night, because stored energy is more important, as the thickness of the flagstone is large. The effect of flagstone thermal inertia and its advantage during the day are illustrated in Figures 6 and 8.

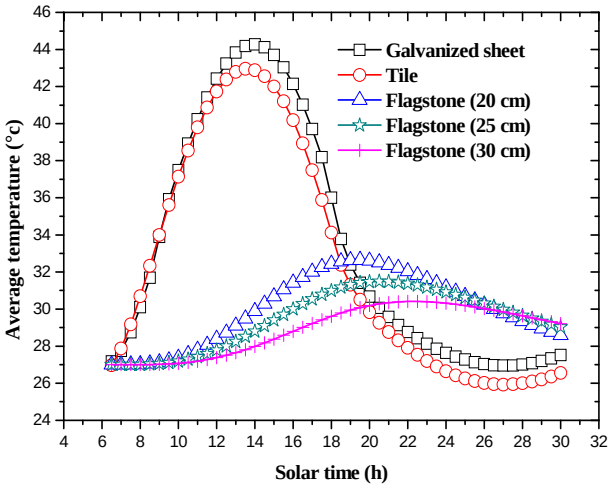

Fig. 6a. Daily variation of indoor air temperatures–theoretical curves.

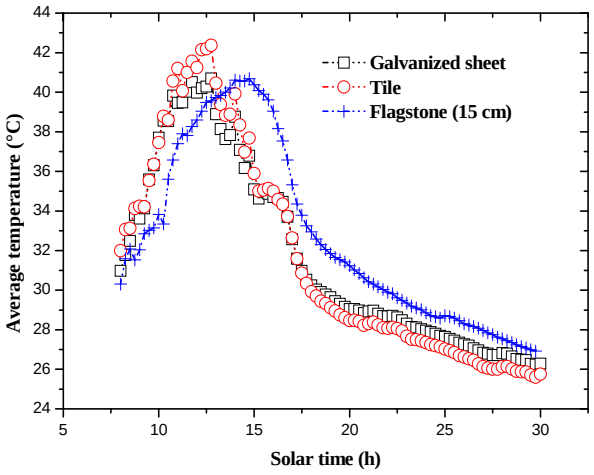

Fig. 6b. Daily variation of indoor air temperatures – experimental curves.

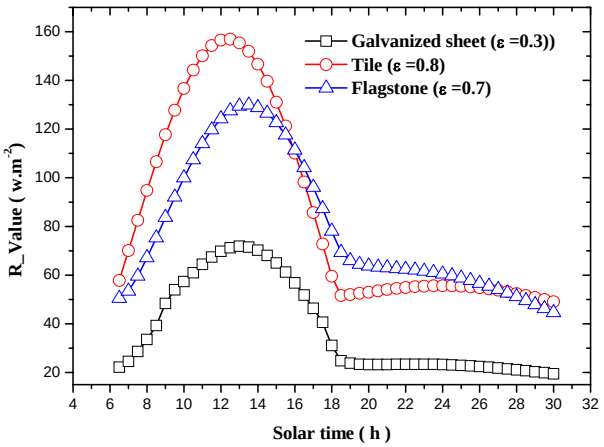

Fig. 7a. Daily variation of thin sheeting roofs radiative heat losses – theoretical curves.

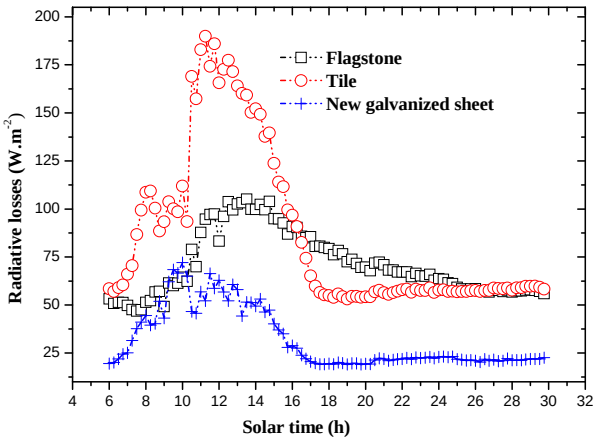

Fig. 7b. Daily variation of thin sheeting roofs radiative heat losses – experimental curves.

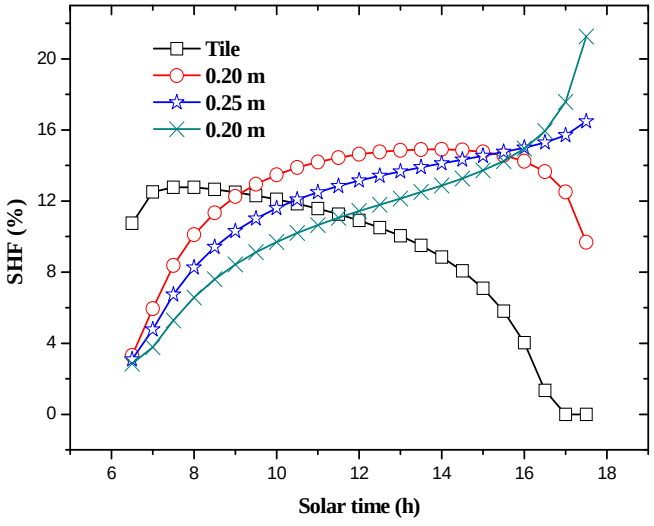

Fig. 8. Daily variation of solar heat gains factor-theoretical curves.

The thermal inertia effects must be more important in the case of reinforced concrete flagstone roofs. Thus, a compromise between the mechanical resistances and heat transfer efficiency must be established for flagstone roofs.

In tropics, modern building roofs generate important heat loads. However, for thermal quality, thin sheeting roof is more interesting at night because of the lager radiant cooling, whereas the flagstone roof is more interesting at daytime. The use of flagstone roofs in our regions has been increasing due to their mechanical resistance properties. Hence the thickness of flagstone roofs must necessarily be optimized by taking into account prevailing climatic conditions. Whatever the choice (thin sheeting or flagstone roofs) it is necessary to use thermal insulation screens in order to reduce solar heat loads and maintain good thermal quality inside the buildings.

The theoretical analysis of the effect of inlet and outlet location of air on buildings' fabrics on indoor air temperature distribution is carried out and shows the importance of building openings' localization on indoor air temperature.

Standard scenarios were considered. Air inlet and outlet have been considered at different zones of the building's fabric as shown on Figure 9. Figure 10 shows the entering and removal air effect on indoor air temperature inside buildings.

The results have shown that among the four scenarios considered, the first case reduces significantly indoor temperatures. Air inlet at floor height and outlet at ceiling height produce a good pattern of air movement, when it is required for cooling. The height between inlet and outlet seems to play an important role in the establishment of the building's thermal comfort during wind-driven ventilation. Its main function is to produce draught during stack-effect ventilation or natural air movement.

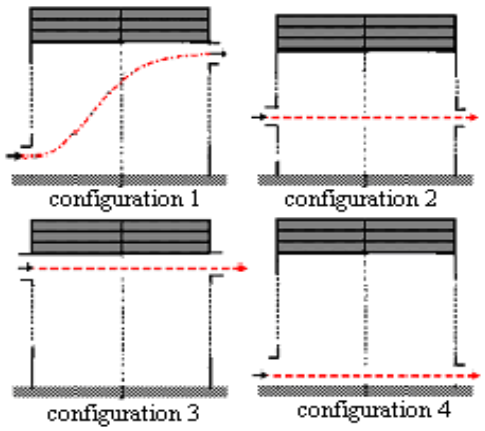

Fig. 9. Schematic view of air inlet and outlet scenarios.

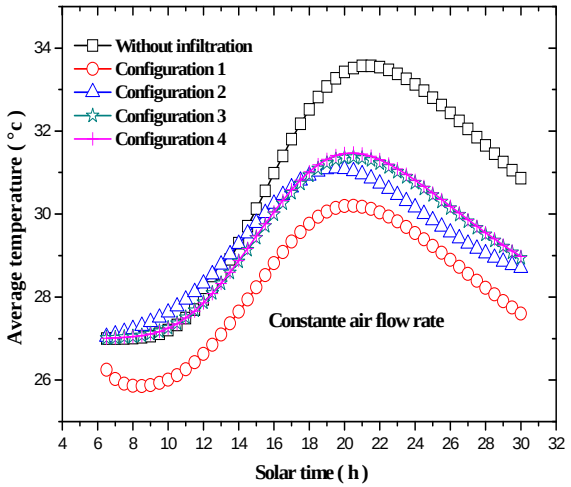

Fig. 10. Daily variation of indoor air temperatures-theoretical curves.

Effect of insulation screens on the building's thermal behaviour

Numerical results obtained for ceiling void insulation screens (even without air flow) plotted in Figure 11 have shown the decreasing indoor temperatures inside the buildings. The ceiling void limits the heat exchange because of the existing air gap. As in previous works [11], the present predicted model allowed to show the importance of air flow rate on the thermal performance of the ceiling void screen.

The effectiveness of this complex roof can be increased by ensuring air ventilation process. In fact, the increase in the air flow rate reduces indoor air temperatures in the room. In attic space, the thickness of the air gap does not have an effect on energy collected per unit on ceiling area. The heat conduction in the air layer is negligible compared to the radiative exchanges. Respectively, Figures 12 and 13a show daily variations of indoor air temperature and solar heat gain factor. The results of these figures indicate that polystyrene and vegetation canopy screens reduce better the heat gains in buildings, compared to thermal performances of plaster false ceiling. Among all these thermal insulation screens, vegetable cover is a screen which reduces better heat gains in buildings.

The experimental results of Figures 13b and 14b have confirmed clearly the predicted results, showing that vegetation cover insulates better than flagstone roofs in spite of its few radiative losses (Figure 15). Plants absorb a significant proportion of solar radiation and seem to be the best thermal insulation screen suitable for flagstone roofs.

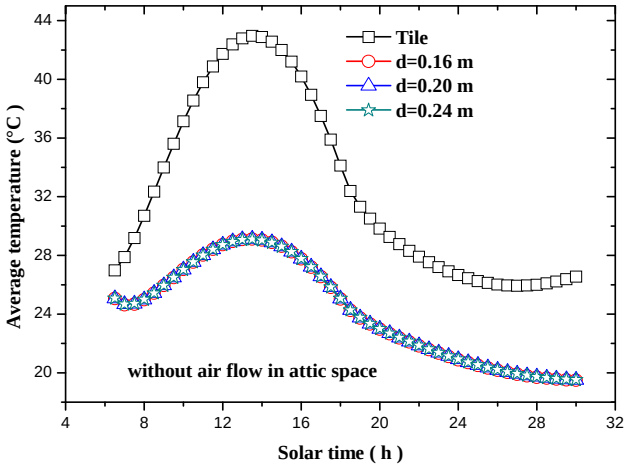

Fig. 11. Attic space effect on indoor air temperatures-theoretical curves.

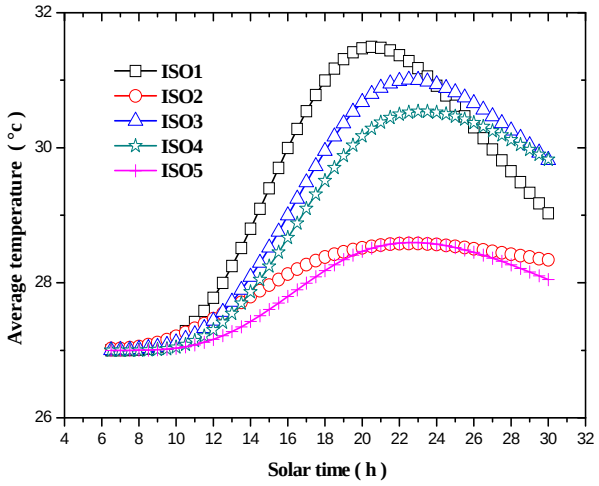

Fig. 12. Insulation screens effect on indoor air temperatures-theoretical curves.

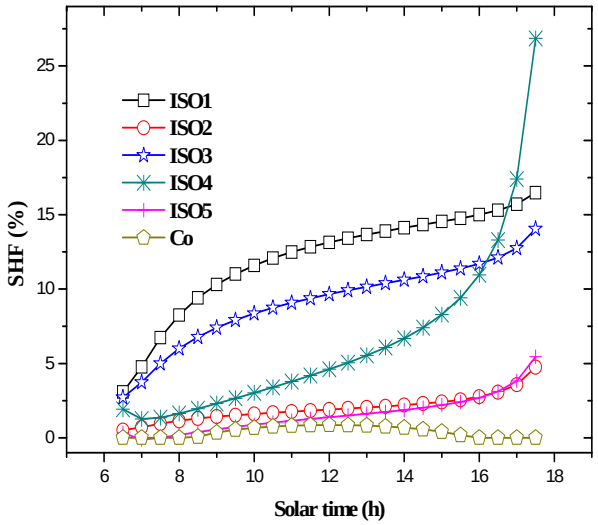

Fig. 13a. Daily variation of solar heat gains factor of various heat insulation screens- theoretical curves.

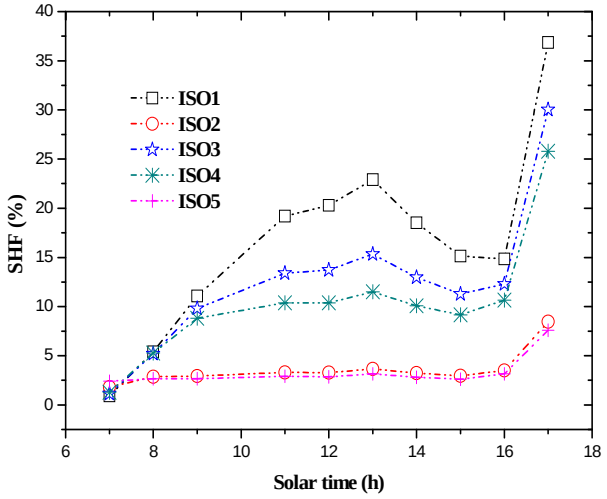

Fig. 13b. Daily variation of solar heat gains factor of various heat insulation screens- experimental curves.

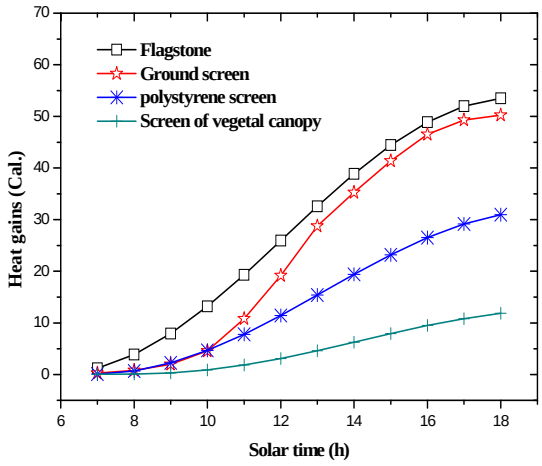

Fig. 14a. Daily variation of heat gains of various insulations screens- theoretical curves.

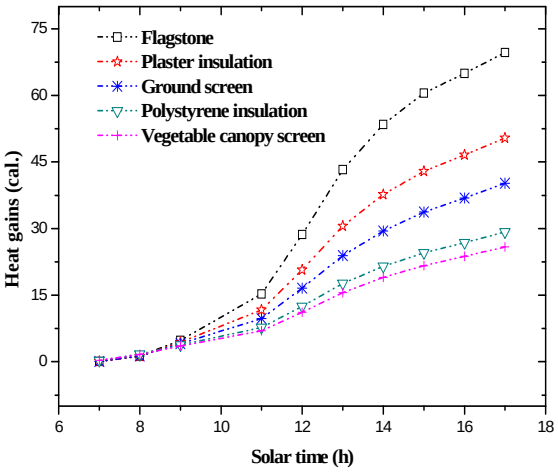

Fig. 14b: Daily variation of heat gains of various insulations screens- experimental curves.

The variation of SHF of the ventilated attic void compared to other thermal insulation screens beneath flagstone in Figure 13a has shown that the ventilated attic seems to be more effective. However, the widespread use of the reinforced concrete flagstone roofs due to its mechanical resistance may lead to the implementation of vegetable cover screens. It is important to determine the flux of heat penetrating the

building which is affected by green roof for various leaf area indices denoting the type or the extent of coverage of the roof. LAI is one of the important parameter affecting the micro-climate of the green canopy and hence the interior of the building. Figure 16 shows the effect of parametric variations in LAI on the indoor air temperature inside buildings. Increase in LAI leads in general to a reduction in coverage area and hence the insulating effect. Results determine that larger LAI reduces indoor air temperature, stabilizes fluctuating values and reduces the penetrating flux. Foliar density optimization and hence the thickness of vegetable must allow the plants' selection for the implementation of green roofs system of buildings in hot-humid tropics.

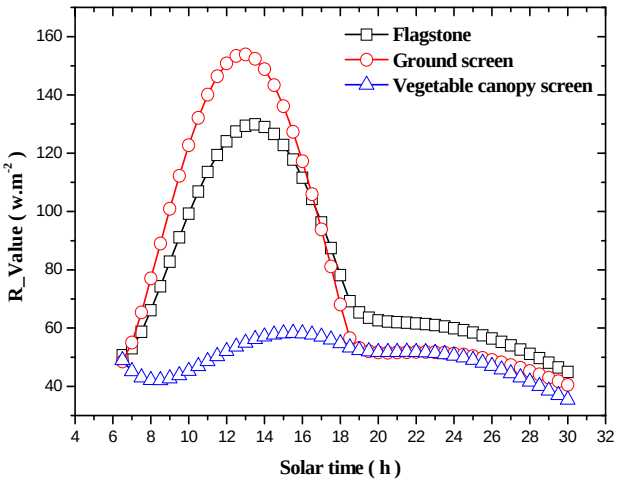

Fig. 15a. Daily variation of radiative heat exchange of various heat insulation screens- theoretical curves.

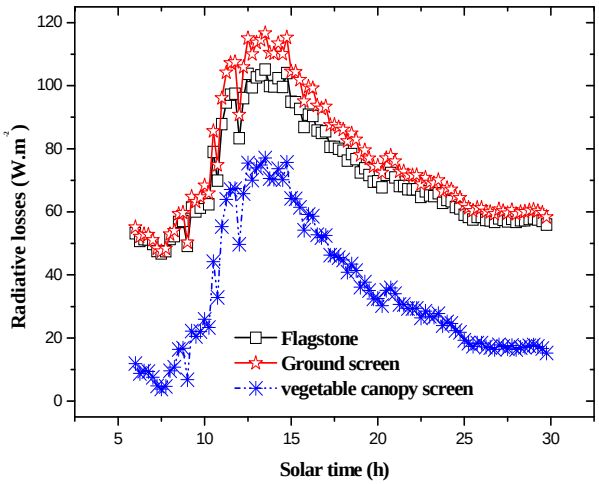

Fig. 15b. Daily variation of radiative heat exchange of various heat insulation screens – experimental curves.

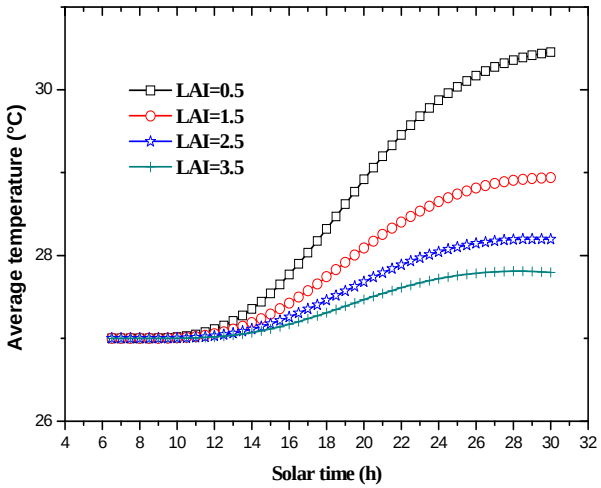

Fig. 16. Leaf Area Index (LAI) effect on indoor air temperature-theoretical curves.

6. CONCLUSION

A numerical model based on an implicit finite-differences method was developed to calculate the time-dependent temperature variation inside buildings. Gauss-Seidel's iterative method is used to resolve linear equations. The models are applied for the simulation and comparison of the thermal characteristics of variants of a typical roof structure of buildings used in hot-humid tropics. The investigation is carried out under variable climatic conditions. Numerical study work is supplemented by an experimental analysis. The results have shown that the thin sheeting roofs induce important thermal loads into buildings during the sunshine period.

They are more interesting during the night because of their large reflectivity, emissivity and their weak thermal inertia. However, attic space for the thin sheeting roofs reduces heat gains and improves thermal quality of the buildings. A more robust and reinforced concrete flagstone roofs limits thermal loads during sunshine period, but they continue to restore energy stored the day even very later in the night, because of the great thermal inertia.

Heat transfers for various insulation screens suitable for flagstone roofs are modelled. The numerical and experimental results obtained show that implemented complex roofs reduce the penetrating flux. The results indicate that bioclimatic insulation screens are more effective than the screens of ground layer, false ceiling in plaster and even the polystyrene plate. Results determine that larger LAI reduces the indoor air

temperature, stabilizes the fluctuating values and reduced the penetrating flux. Foliar density optimization and hence the thickness of vegetable must allow the plants' selection in the implementation of green roofs system of buildings in hot-humid tropics.

It is recommended that future studies should include the economic side of the problem, moisture transport and condensation in roof selections under hot-humid tropics climatic conditions as well.

NOMENCLATURE

d	Attic space thickness (m)
e	Roof thickness (m)
e_j	Thickness of the j-th layer (m)
G_j	j-th layer conductance ($W.K^{-1}$)
H	Indoor height of patio (m)
h_j	Convective heat-transfer coefficient on j-th layer of air ($W.m^{-2}K^{-1}$)
h_{ae}	Convective heat-transfer coefficient on roofs ($W.m^{-2}K^{-1}$)
h_{rae}	Radiative heat-transfer coefficient between roofs and the sky ($W.m^{-2}K^{-1}$)
h_{rN0}	Radiative heat-transfer coefficient between roofs and the ceiling ($W.m^{-2}K^{-1}$)
h_{rN}	Radiative heat-transfer coefficient between roofs and the floor ($W.m^{-2}K^{-1}$)
LAI	Leaf Area Index (-)
L_V	Latent heat of evaporation ($J.Kg^{-1}$)
$\dot{m}$	Air flow rate ($Kg.s^{-1}$)
N0	Number of sublayer of complex roof (-)
Nu	Nusselt number (-)
P_V	Partial vapor pression (Pa)
P_{VS}	Saturation Vapor pression (Pa)
Q	Heat gains (cal.)
r_i	Mean stomatal resistance (sm^{-1})
r_e	Mean canopy resistance to sensible heat transfer (sm^{-1})
RH	Relative humidity (-)
R-value	Roof radiative heat exchange (Wm^{-2})
R_{th}	Thermal resistance (Wm^{-2})
S	Surface (m^2)
SHF	Solar Heat Factor (%)
t	Time (s)
T_j	j-th node temperature (K)
Ta	Ambient temperature (K)
T_{dp}	Temperature of the dew point (K)
x	Spatial axis (m)

Initials

Co	Ventilated ceiling void
ISO1	Simple reinforced concrete flagstone
ISO2	Reinforced flagstone insulated by polystyrene plate
ISO3	Reinforced flagstone insulated by false ceiling in plaster
ISO4	Reinforced flagstone insulated by ground layer
ISO5	Reinforced flagstone insulated by bioclimatic vegetation cover

Greek letters

$(\rho c_p)_j$	j-th layer specific heat ($J.m^{-3}K^{-1}$)
α	Roof absorptivity coeficient (-)
ε_{sky}	Sky' emissivity coefficient (-)
ε_{roof}	Roof' emissivity coefficient (-)
ε_p	Vegetation canopy porosity (-)
λ	Thermal conductivity ($Wm^{-1}K^{-1}$)
σ	Boltzmann-Stefan constant ($\sigma = 5.67\ 10^{-8}$) ($W.m^{-2}K$)
ϕ_β	Incident solar energy density (Wm^{-2})
ϕ_e	Transmitted solar energy density (Wm^{-2})

Subscripts

J	node index
e	inlet
s	outlet

REFERENCES

[1] Nahar, N.M., Sharma P., and Purohit, M.M., 1999. Studies on solar passive cooling techniques for arid areas. *Energy Conversion and Management* 40: 89-95.

[2] Tang, R., and Y. Etzion, 2004. On thermal performance of an improved roof pond for cooling buildings. *Building and Environment* 39: 201-209.

[3] Dilip, J., 2006. Modeling of solar passive techniques for roof cooling in arid regions. *Building and Environment* 41: 277-287.

[4] Xuxu, Y., and Zhanget., 2005. Modeling and simulation on the thermal performance of shape stabilized phase change material floor used in passive solar buildings. *Energy and Buildings* 37: 1084-1091.

[5] Miranville, F., Boyer, H., and Garde, F., 2003. On thermal behaviour of roof-mounted radiant barriers under tropical and humid climatic conditions: modeling and empirical validation. *Energy and Buildings 35: 997-1008.*

[6] Kumar, R., and S.C. Kaushik, 2005.Performance evaluation of green roof and shading for thermal protection of buildings *Building and Environment* 40: 1505-1511.

[7] Saighi, M., and M. Christian, 1998. A simplified model of heat and mass transfer in soil-plant-atmosphere system. *International Journal on Heat Mass and Transfer* 41(11): 1459-1471.

[8] Dimoudi, A., and A. Androutsopoulos, 2006. The cooling performance of a radiator based roof component. *Solar Energy* 80: 1039-1047.

[9] Tang, R., Meir, I.A., and Wu, T., 2006. Thermal performance of non-conditioned buildings with vaulted roofs in comparison with flat roofs. *Building and Environment* 41: 268-276.

[10] Sami, A.S. 2002. Thermal performance of building roof elements. *Building and Environment* 37: 665-675.

[11] Saraka, J.K. 1999. Typology study of the solar heat gains of building's fabric in tropical and humid regions. Ph.D. dissertation, Polytechnic institute of Grenoble, France [in French language].